Crystallization of catalytic CVD hydrogenated n-a-Si films on textured glass substrates by flash lamp annealing

Zheng Wang[1], Huynh Thi Cam Tu[1], and Keisuke Ohdaira[1]

[1]*Japan Advanced Insistute of Science and Technology, 1-1 Asahidai, Nomi, Ishikawa 923-1292, Japan*

E-mail: ohdaira@jaist.ac.jp

Flash lamp annealing (FLA) is a short-duration annealing technique and can crystallize amorphous silicon (a-Si) films for thin-film polycrystalline Si (poly-Si) solar cells. We investigated the crystallization of n-type hydrogenated a-Si (n-a-Si:H) films formed by catalytic chemical vapor deposition (Cat-CVD) on Si nitride- (SiN_x-) coated textured glass substrates. The n-a-Si:H films with a thickness of ~2.7 μm were crystallized by FLA with no film peeling even without chromium adhesion layers. We also confirmed that the crystallization takes place through explosive crystallization (EC). The addition of phosphorous to the precursor a-Si:H slightly modifies the crystallization, resulting in different grain size and EC velocity compared to the case of EC of intrinsic a-Si:H.

I. Introduction

The use of solar energy has always been a priority in order to solve environmental issues. Of a wide variety of solar cells, wafer-based crystalline silicon (c-Si) solar cells have been utilized most widely. However, the problems of Si material usage in great quantities and high fabrication cost need to be solved. Thin-film polycrystalline Si (poly-Si) solar cells, expected to be one of the future low-cost solar cells, require only a few μm of Si material.[1–14] The current world record power conversion efficiency of the thin-film poly-Si solar cell on glass substrate with a back-contact structure exceeds 15%.[13]

We have thus far demonstrated the formation of intrinsic poly-Si (i-poly-Si) films by crystallizing precursor hydrogenated intrinsic amorphous Si (i-a-Si:H) films by flash lamp annealing (FLA) on glass substrates with chromium (Cr) adhesion layers.[15] Cr films act as adhesion layers to suppress Si films peeling by FLA. On the other hand, Cr impurities introduce into poly-Si and enhance carrier recombination, by which the solar cell performance is degraded. For the cells fabricated with a back-contact structure, metal films between glass and poly-Si will not be necessary.[14]

We have attempted to use precursor a-Si films formed by various types of deposition methods, such as catalytic chemical vapor deposition (Cat-CVD), sputtering, and electron-beam (EB) evaporation.[15–24] The crystallization of EB-evaporated a-Si films on flat glass substrates is driven by liquid-phase explosive crystallization (EC), which leads to the formation of crystal grains with a size of several tens of μm.[17] Different type of EC occurs for the crystallization of Cat-CVD a-Si:H films, through which two types of regions with different microstructures appear alternately in the direction of crystallization with a period of ~1 μm.[16] This is due to the alternative emergence of liquid-phase epitaxy (LPE) and solid-phase nucleation (SPN).[16,17] One of the problems for the crystallization

of Cat-CVD a-Si:H by FLA is the peeling of Si films during the crystallization in the case without a Cr adhesion layer due to the existence of hydrogen. To solve this problem, we attempt to enhance anchor effect by forming texture patterns on glass surfaces by reactive ion etching (RIE). We previously found that EB-evaporated a-Si films on glass substrates textured by RIE can be crystallized through EC depends on the roughness of glass surfaces.[21,22] Similar crystallization and anchor effect can also be seen when a Si nitride (SiN_x) film is inserted between a-Si and textured glass, which will act as passivation and anti-reflection (AR) films for the back-contact cell.[22]

In this study, we attempted to crystallize Cat-CVD a-Si:H films by FLA on SiN_x-coated textured glass substrates. We particularly used n-type a-Si:H films as precursors aiming at the clarification of the effect of phosphorous (P) addition to a-Si:H on their crystallization, because doped absorber layers should be used in the actual thin-film poly-Si solar cells.

2. Experimental Procedures

19.8 × 19.8 × 0.7 mm^3-sized glass substrates (Corning Eagle XG) were ultrasonically cleaned in Semico clean 56, ethanol, and deionized water for 10 minutes, respectively. We then formed texture patterns on the glass substrates by RIE for 2.5 hours using CF_4 gas at a flow rate of 30 sccm, a pressure of 2.6 Pa, and a radio frequency (RF) power of 200 W. The surface root-mean-square (RMS) roughness of the glass substrates was measured by atomic force microscopy (AFM). The RMS roughness of a glass substrate before RIE was <5 nm, while it increased to 90–110 nm by the RIE treatment.

80-nm-thick SiN_x films were deposited on the textured glass substrates by Cat-CVD at a catalyzer temperature (T_{cat}) of 1750 °C, a substrate holder temperature (T_{sub}) of 350 °C,

a pressure of 3.2 Pa, and gas flow rates of SiH_4 and NH_3 of 4 and 250 sccm, respectively. We then deposited ~2.7-μm-thick i-a-Si:H and n-a-Si:H films by Cat-CVD at a T_{cat} of 1800 °C, a pressure of 1.1 Pa, and gas flow rates of SiH_4, H_2, and He-diluted 2.32% PH_3 of 50, 10, and 0 or 0.02 sccm, respectively. Hydrogen contents in the SiN_x and a-Si:H films, measured by Fourier-transform infrared spectroscopy, were ~3–4 %. FLA was performed for the n-a-Si:H films at fluences of 15.9–16.7 J/cm^2, pulse duration of 7 ms, sub-pulse frequency of 1–10 kHz, and a preheat temperature of 500 ℃ in argon (Ar) atmosphere. Note that hydrogen effusion from a-Si:H films during FLA is negligible,[20] and similarly, hydrogen in SiN_x is expected to remain there after FLA. Hydrogen in the SiN_x films will thus not affect the crystallization of a-Si:H films. Figure 1 shows the schematic cross-sectional view of the sample. The sub-pulse emission leads to the periodic change of Si temperature during FLA and resulting formation of macroscopic stripe patterns on a poly-Si surface if EC takes place.[18,19] The velocity of EC (v_{EC}) was estimated from the width of the macroscopic stripe patterns and inverse of sub-pulse frequency.[18,19] The crystallization and crystalline fraction of Si films were characterized by Raman spectroscopy. The cross-sectional microscopic image of a poly-Si was observed by transmission electron microscopy (TEM). A focused-ion beam (FIB) micro-sampling technique was used to prepare the cross-section of a poly-Si film for the TEM observation.

3. Results and discussion

Figure 2 shows the Raman spectra measured the spectra at three points, labeled a, b and c as indicated in the inset, on surface of i- and n-poly-Si films after FLA. The black dashed line is the spectrum of a c-Si wafer used as a reference. All the spectra contain a

strong peak around 520 cm^{-1} derived from c-Si phase, while a peak located at 480 cm^{-1}, from a-Si phase, is not clearly seen. These imply the Si films are sufficiently crystallized by the irradiation of a flash-lamp pulse. The n-poly-Si films show a relatively low (519.3 cm^{-1}) c-Si peak, indicating the existence of the tensile stress.[23)] The a-Si films deposited at 450 °C is compressively stressed, and the stress reduces at lower deposition temperature.[23,24)] Despite the compressive stress in Cat-CVD a-Si:H films, the compressive stress in the poly-Si is reduced during FLA, resulting in a tensilely-stressed poly-Si surface. [23,24)] c-Si peaks have a full width at half maximum (FWHM) of 7.6–9.6 cm^{-1}, indicating that the n-poly-Si films are composed of fine grains.[25)] The crystalline fraction of the n-poly-Si films was estimated to be 0.78–0.98, which is lower than that of the i-poly-Si films of 0.88–0.98. The smaller crystalline fraction of the poly-Si films may be due to P dopants interfering the rearrangement of Si atoms during the crystallization process.[26)] It should be emphasized that no Si film peeling occurs even without the use the Cr adhesion layer. By forming textured structures on the glass surfaces, adhesion between poly-Si and SiN_x-coated glass is enhanced due to the increased interface area, which contributes to the suppression of Si film peeling and the crystallization of the entire surfaces. Since the precursor a-Si:H films were deposited at a high T_{sub} of 450 °C, it is expected to obtain the poly-Si films with a low defect density.[27)] In addition, due to the passivation effect of the SiN_x film and the absence of the Cr adhesion layer, the thin-film poly-Si solar cells with higher conversion efficiency than those on Cr films will be obtained.[21)]

Figure 3 shows the surfaces of i- and n-poly-Si films on SiN_x-coated textured glass after FLA at sub-pulse emission frequencies of 1, 2, 4, 6 and 10 kHz, respectively. All the samples have macroscopic stripe patterns and the width of the stripe changes with

sub-pulse emission frequency. The formation of the macroscopic stripe patterns is related to the modulation of the temperature of Si films during millisecond treatment due to discrete sub-pulses.[18,19] These clear experimental evidences indicate that the crystallization of Cat-CVD a-Si:H films by FLA on SiN_x-coated textured glass substrates takes place by EC, lateral crystallization induced by the release of latent heat due to the enthalpy difference between a-Si and c-Si and its diffusion.[28]

Figure 4 shows the widths of stripes formed on i- and n-poly-Si films as a function of the inverse of the frequency of sub-pulse emission. Linear relations between them are clearly seen, and their slopes yield the lateral v_{EC} of the a-Si films.[18,19] The v_{EC} of i-a-Si:H films deposited on Cr-coated flat glass substrates by Cat-CVD is ~4 m/s, while the EB-evaporated i-a-Si films shows a v_{EC} of ~14 m/s, equivalent to the LPE velocity of molten Si near the melting point of a-Si.[18,19,29] However, the v_{EC} of n-a-Si:H deposited on SiN_x-coated textured glass substrates by Cat-CVD is in between them. This implies the emergence of EC with different mechanisms. One possible reason is that P dopants affect the crystallization rate and grain growth.[30,31]

Figure 5 shows the cross-sectional TEM image of n-poly-Si films formed by FLA on textured glass. One can see small grains, large stretched grains, and a number of voids in the vicinity of the surface. We have previously found that the EC of i-a-Si:H films by FLA forms the periodic microstructure consisting of LPE-based EC regions and solid-phase crystallization (SPC) regions.[16] However, the cross-sectional TEM image of the n-poly-Si film contains no such periodic microstructures. This implies the emergence of different EC mechanisms. The particular EC of n-a-Si:H films might be related to P dopants. The addition of P dopants can accelerate both SPC and LPE [30,31]. This may also explain that the v_{EC} of n-a-Si films is significantly higher than the v_{EC} of the i-a-Si:H films.

Of course, we should also take into account the effects of SiN_x underneath the Si films and textured glass surfaces, which are different from our previous structures with Cr-coated flat glass, on the EC mechanism and resulting microstructure of poly-Si. Nevertheless, we consider the existence of P dopants affects the EC mechanism more dominantly, since the i-poly-Si films formed on SiN_x-coated textured glass shows the same v_{EC} as those formed on Cr-coated flat glass substrates, as shown in Fig. 4.

We will fabricate and evaluate the thin-film solar cells on glass substrate using n-poly-Si formed by FLA of n-a-Si:H films in the future. It is necessary to realize efficient light collection and the suppression of carrier recombination for solar cells with a high conversion efficiency. The use of SiN_x contributes to the anti-reflection and passivation for the n-poly-Si solar cells.

4. Conclusion

The FLA was performed on Cat-CVD i- and n-a-Si:H films deposited on SiN_x-coated textured glass substrates to form the i- and n-poly-Si films with no film peeling even without Cr adhesion layers. The textured glass surface plays a role in enhancing the anchor effect and suppressing the peeling of Si film, while SiN_x film acts as the poly-Si surface passivation and anti-reflection film for the thin-film solar cells with a back-contact structure. It is confirmed that the crystallization mechanism of the n-a-Si:H films on the SiN_x-coated textured glass substrate is based on EC. The addition of P atoms to a-Si:H films affects the grain size and EC velocity. The obtained n-poly-Si is expected to be utilized as a high-quality absorber of the back-contact thin-film solar cells.

Acknowledgements

This work is partly supported by JSPS Bilateral Program, Grant number JPJSBP120193511.

Reference

1) W. Fuhs, S. Gall, B. Rau, M. Schmidt, and J. Schneider, Sol. Energy **77**, 961 (2004).
2) A. A. D. T. Adikaari, N. K. Mudugamuwa, and S. R. P. Silva, Sol. Energy Mater. Sol. Cells **92**, 634 (2008).
3) J. K. Saha, K. Haruta, M. Yeo, T. Koabayshi, and H. Shirai, Sol. Energy Mater. Sol. Cells **93**, 1154 (2009).
4) K. R. Catchpole, M. J. McCann, K. J. Weber, and A. W. Blakers, Sol. Energy Mater. Sol. Cells **68**, 173 (2001).
5) D. Amkreutz, J. Müller, M. Schmidt, T. Hänel, and T. F. Schulze, Prog. Photovolt: Res. Appl. **19**, 937 (2011).
6) T. Matsuyama, M. Tanaka, S. Tsuda, S. Nakano, and Y. Kuwano, Jpn. J. Appl. Phys. **32**, 3720 (1993).
7) M. Spitzer, J. Schewchun, E. S. Vera, and J. J. lofersky, Proc. 14th IEEE PV Specialists Conf., p. 375 (1980).
8) R. Kakkad, J. Smith, W. S. Lau, S. J. Fonash, and R. Kerns, J. Appl. Phys. **65**, 2069 (1989).
9) R. Kakkad, G. Liu, and S. J. Fonash, J. Non. Cryst. Solids. **115**, 66 (1989).
10) C. T. Trinh, N. Preissler, P. Sonntag, M. Muske, K. Jäger, M. Trahms, R. Schlatmann, B. Rech, and D. Amkreutz, Sol. Energy Mater. Sol. Cells **174**, 187 (2018).

11) Y. Yogoro, A. Masuda, and H. Matsumura, Thin Solid Films **430**, 296 (2003).

12) F. L. Bregolin, K. Krockert, S. Prucnal, L. Vines, R. Hübner, B. G. Svensson, K. Wiesenhütter, H.-J. Möller, and W. Skorupa, J. Appl. Phys. **115**, 064505 (2014).

13) S. Garud, C. T. Trinh, D. Abou-Ras, Bernd Stannowski, R. Schlatmann, B. Rech, and D. Amkreutz, Sol. RRL **4**, 2000058 (2020).

14) N. Preissler, D. Amkreutz, P. Sonntag, M. Trahms, R. Schlatmann, and B. Rech, Sol. RRL **1**, 1700015 (2017).

15) K. Ohdaira, Y. Endo, T. Fujiwara, S. Nishizaki, and H. Matsumura, Jpn. J. Appl. Phys. **46**, 7603 (2007).

16) K. Ohdaira, T. Fujiwara, Y. Endo, S. Nishizaki, and H. Matsumura, J. Appl. Phys. **106**, 044907 (2009).

17) K. Ohdaira and H. Matsumura, J. Cryst. Growth **362**, 149 (2013).

18) K. Ohdaira, N. Tomura, S. Ishii, and H. Matsumura, Electrochem. Solid-State Lett. **14**, H372 (2011).

19) K. Ohdaira, Can. J. Phys., **92**, 718 (2014).

20) K. Ohdaira, H. Takemoto, K. Shiba, and H. Matsumura, Appl. Phys. Express **2**, 061201 (2009).

21) K. Kurata and K. Ohdaira, Jpn. J. Appl. Phys. **58**, SBBF10 (2019).

22) A. Yago and K. Ohdaira, Thin Solid Films **728**, 138681 (2021).

23) K. Ohdaira, Thin Solid Films **575**, 21 (2015).

24) T. Watanabe and K. Ohdaira, Thin Solid Films **595**, 235 (2015).

25) C. Smit, R. A. C. M. M. van Swaaij, H. Donker, A. M. H. N. Petit, W. M. M. Kessels, and M. C. M. van de Sanden, J. Appl. Phys. **94**, 3582 (2003).

26) T. Nishikawa, K. Ohdaira, and H. Matsumura, Curr. Appl. Phys. **11**, 604 (2011).

27) T. Nozawa and K. Ohdaira, Int. J. Mater. Res. **108**, 827 (2017).

28) H.-D. Geiler, E. Glaser, G. Götz, and M. Wagner, J. Appl. Phys. **59**, 3091(1986).

29) M. Smith, R. McMahon, M. Voelskow, D. Panknin, and W. Skorupa, J. Cryst. Growth **285**, 249 (2005).

30) M. D. Efremov, V. A. Volodin, S. A. Arzhannikova, S. A. Kochubeĭ, and V. N. Ulasyuk, Tech. Phys. Lett. **31**, 128 (2005).

31) J. F. Pierson, K. S. Kim, J. Jolly, and D. Mencaraglia, J. Non-Cryst. Solids. **270**, 91 (2000).

Figure Captions

Figure 1 (Color online) Schematic cross-sectional view of the sample.

Figure 2 (Color online) Raman spectra of Si films after FLA. (a), (b), and (c) shown in the inset indicate measurement points of Raman spectra. Dash and solid lines exhibit the spectra of i- and n-poly-Si, respectively. The Raman spectra of the poly-Si films were normalized by the intensity of c-Si peaks. The spectrum of a c-Si wafer is also shown as a black dash line for comparison.

Figure 3 (Color online) Surfaces of i- and n-poly-Si films after FLA with sub-pulse frequencies of 1, 2, 4, 6 and 10 kHz.

Figure 4 (Color online) Width of macroscopic stripe patterns on i- and n-poly-Si films as a function of the reciprocal of sub-pulse emission frequency. The straight lines are the results of line fitting.

Figure 5 (Color online) Cross-sectional TEM image of an n-poly-Si film. The cross-section was formed along an EC direction. The poly-Si film was formed by FLA at a sub-pulse emission frequency of 6 kHz.

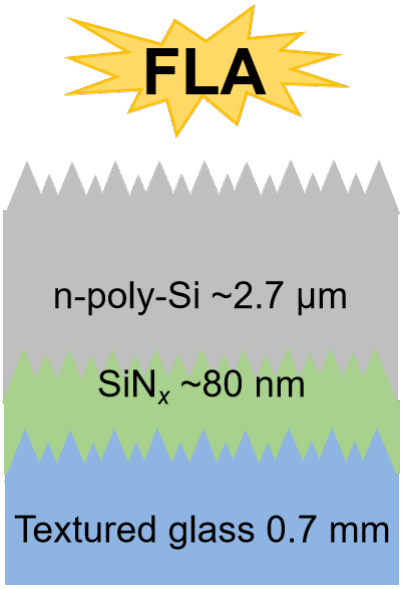

Figure 1 Z. Wang et al.,

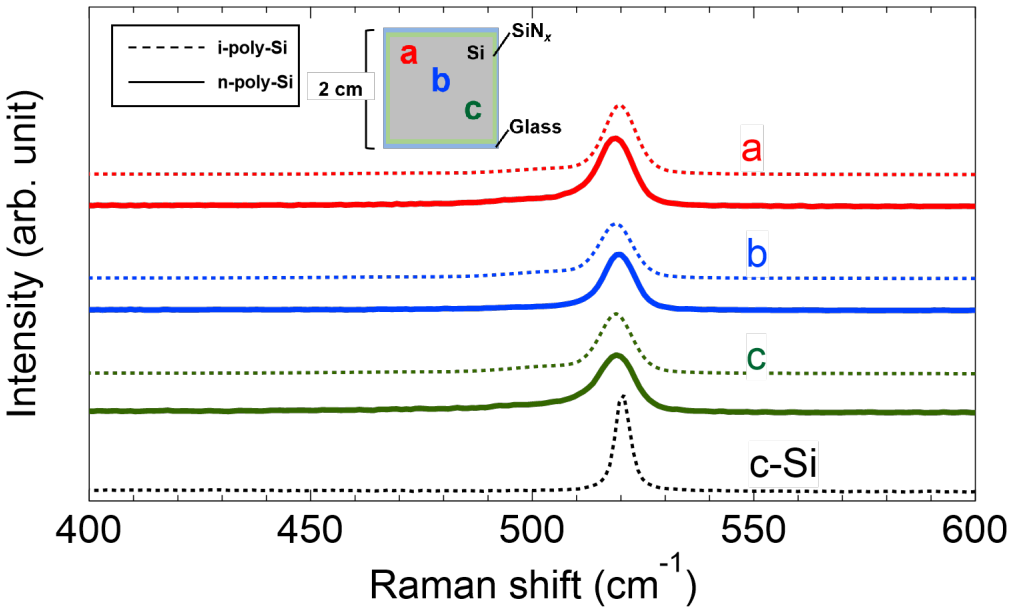

Fig. 2 Z. Wang et al.,

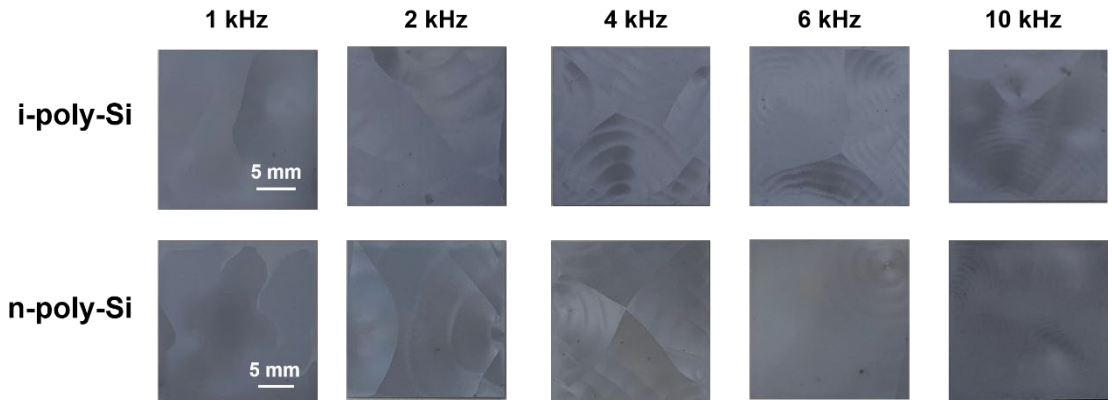

Fig. 3 Z. Wang et al.,

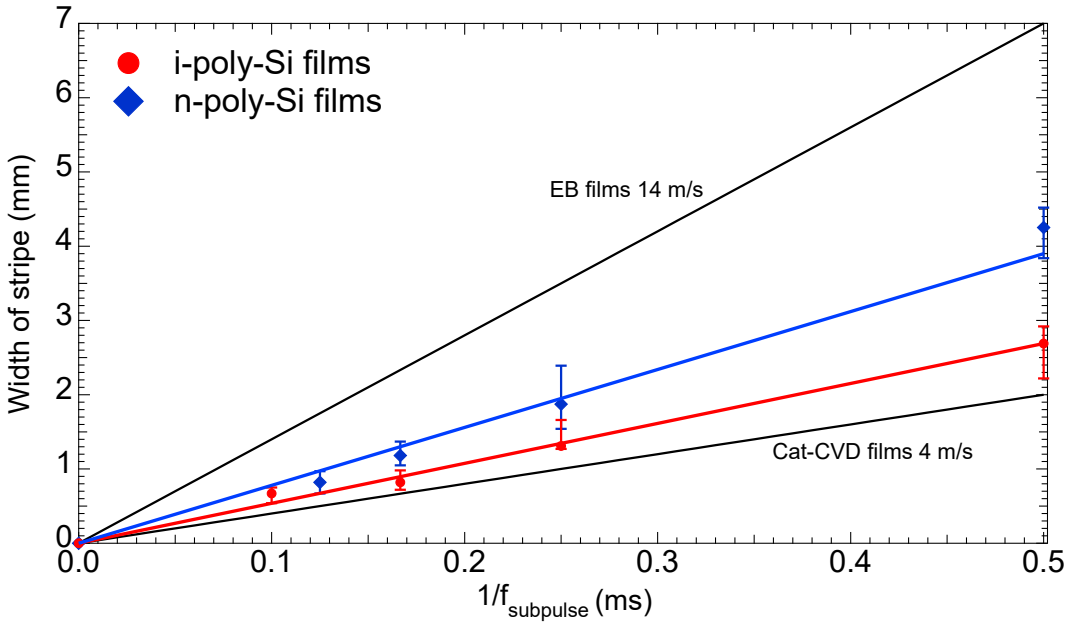

Fig. 4 Z. Wang et al.,

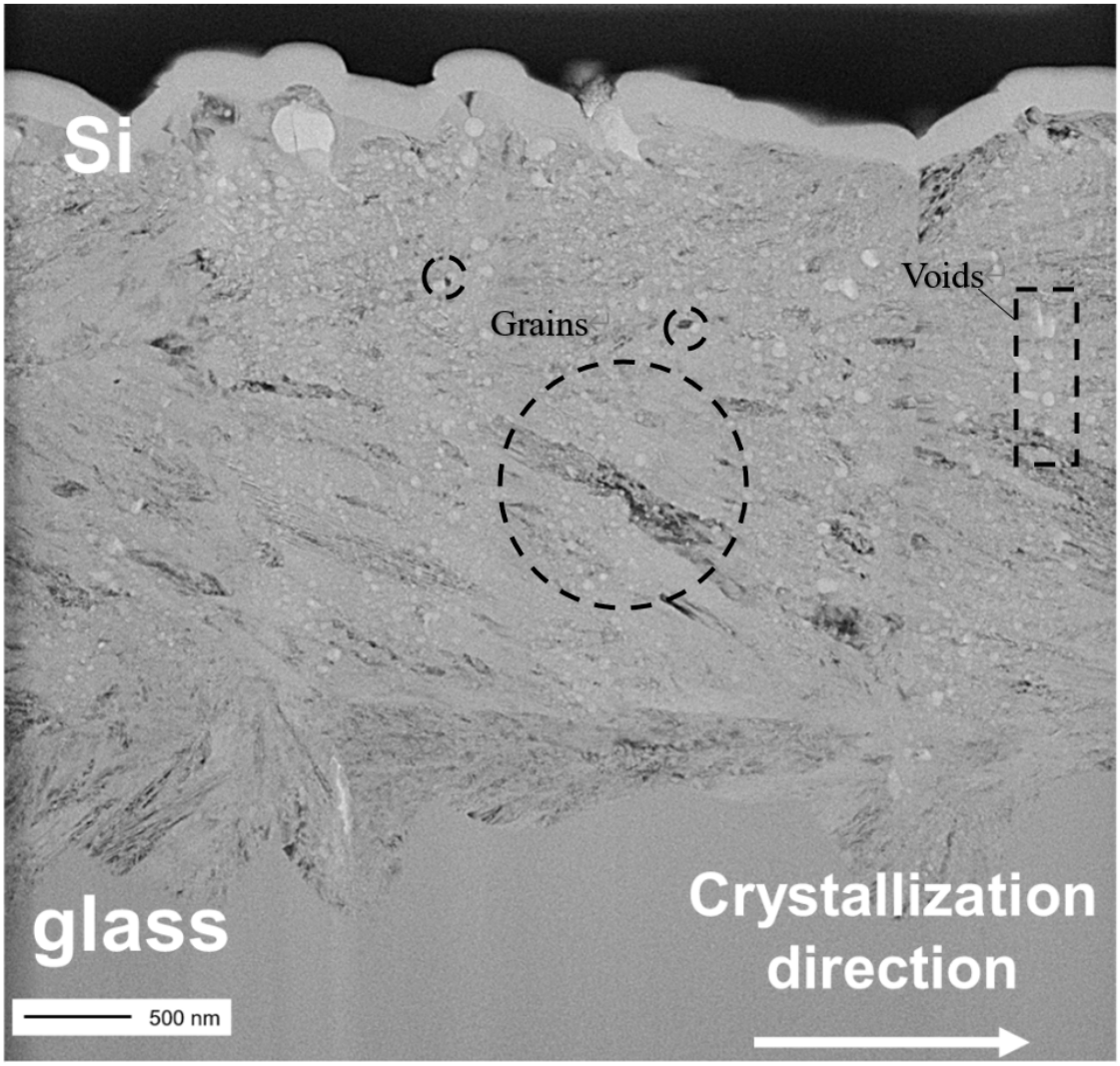

Fig. 5 Z. Wang et al.,